

Direct Estimation of Valence Electron Distribution Around an Ion in Liquid Metals

著者	Waseda Yoshio, Tamaki Shigeru, Takeda Shin'ichi
journal or publication title	Science reports of the Research Institutes, Tohoku University. Ser. A, Physics, chemistry and metallurgy
volume	36
number	2
page range	171-186
year	1992-03-25
URL	http://hdl.handle.net/10097/28374

**Direct Estimation of Valence Electron Distribution
Around an Ion in Liquid Metals***

Yoshio Waseda, Shigeru Tamaki** and Shin'ichi Takeda***

Research Institute of Mineral Dressing and Metallurgy (SENKEN)

(Received January 31, 1992)

Synopsis

Liquid metals consist of ions and electrons. However, the bare ions in liquid metals are recognized to be partially screened by electrons so as to produce the effective ion-ion potential of the long-range oscillatory type and then liquid metals are likely the binary mixtures of ions with some electrons for partial screening and the valence electrons giving a strongly coupled plasma. An attempt is made in this paper to present the valence electron distribution around an ion in liquid metals. The principle of a new method for estimating such information in liquid metals from measured structural data has been described with some selected examples.

1. Introduction

Liquid metals in their pure states have now well-known to be binary mixtures of ions and conduction electrons giving a strongly coupled plasma [1]. Based on this concept, it was pointed out that the structure of liquid metals should be explicitly described by three types of correlations; for ion-ion, electron-electron and ion-electron pairs [2,3]. X-ray and neutron diffraction studies on the structure of liquid metals are good clues to reveal these correlations for the following reasons. Neutrons scatter only on nuclei of the center of ions. Whereas, X-rays scattering experiment also provides the distribution of ions, but it is known to be obtained through the scattering on electrons surrounding ions. Such differ-

* 92-R5th Report of the Research Institute of Mineral Dressing and Metallurgy.

** Permanent address: Department of Physics, Faculty of Science, Niigata University, Niigata 950-21.

*** Permanent address: College of general Education, Kyushu University, Fukuoka 810.

ences in the scattering mechanism in x-ray and neutrons suggest that small but a certain difference should be observed in the structural data measured by two scattering methods. Egelstaff, March and McGill [4] in 1974 first indicated this point, but their suggestion was explicitly cited very recently, mainly due to the limited experimental accuracy of the neutron results for liquid metals [5-7].

Several efforts have been devoted to estimate these three correlations in liquid metals and then recent diffraction experiments on liquid metals with sufficiently quantitative accuracy of X-ray s and neutrons enable us to extract the ion-electron correlations when coupled with the theoretical values for the electron-electron correlations [8]. Such investigation has been extensively made by the present authors as reported in a serial work [9-14].

The main purpose of this paper is to review the systematic information of the valence electron distribution around an ion in liquid metals estimated directly from structural data.

2.Theoretical Background

Let us consider a liquid metal containing N ions and zN valence electrons, where z is the number of valence electrons per atom. In other words, the core electrons are excluded here. When we use the Ashcroft-Langreth form [13,14] of the partial structure factors, the coherent x-ray scattering intensity, $I_X^{\text{coh}}(Q)$, for $Q \neq 0$ is given as follows [15].

$$I_x(Q)/N = [(f_i(Q))^2 S_{ii}(Q) + 2z^{1/2} f_i(Q) S_{ie}(Q) + z S_{ee}(Q)] + (Z-z) S_i^{\text{inc}}(Q), \quad (1)$$

where $f_i(Q)$ is the form factor of an ion (International Tables for X-ray Crystallography [16]), Z the atomic number and z the number of valence electrons. $S_{ii}(Q)$, $S_{ee}(Q)$ and $S_{ie}(Q)$ are the partial structure factors of ion-ion, electron-electron and ion-electron pairs, respectively. $S_i^{\text{inc}}(Q)$ is the incoherent scattering factor of ions. The form factor of a valence electron is considered to be unity, because each valence electron is sufficiently a point charge as a good approximation [4].

The static structure factor of valence electrons, $S_{ee}(Q)$, is also given by the following [15],

$$S_{ee}(Q) = \frac{|\rho(Q)|^2}{z} S_{ii}(Q) + S_{ee}^{(0)}(Q), \quad (2)$$

where $\rho(Q)$ is the Fourier transform of the charge density of valence electrons and $S_{ee}(Q)$ is the structure factor of uniformly distributed electrons [1,8]. Thus, the coherent X-ray scattering intensity of eq.(1) is rewritten in the form,

$$I_x(Q)/N=[f_i(Q)+\rho(Q)]^2 S_{ii}(Q)+zS_{ee}^{(0)}(Q)+(Z-z)S_i^{\text{inc}}(Q). \quad (3)$$

Since $(Z-z)S_i^{\text{inc}}(Q)$ denotes the Compton scattering factor of ions and it could be eliminated from measured intensity and the structure factor of uniformly distributed electrons, $S_{ee}^{(0)}(Q)$, is known to have insignificant contribution to the coherent X-ray scattering, we may obtain the coherent X-ray scattering intensity determined directly from measured intensity data in the following form,

$$I_x^{\text{coh}}(Q)/N=[f_i(Q)+\rho(Q)]^2 S_{ii}(Q), \quad (4)$$

$$=(f_i(Q))^2 S_{ii}(Q)+2z^{1/2}f_i(Q)S_{ie}(Q)+(\rho(Q))^2 S_{ii}(Q). \quad (4')$$

Except for very light elements such as lithium and beryllium, the last term of eq.(4') is negligibly small compared with the first and second terms where the atomic number of liquid metals of interest is not so small. This is quantitatively confirmed by the cases of several liquid metals [9-11]. Then, eq.(4') can be approximated to,

$$I_x^{\text{coh}}(Q)/N=(f_i(Q))^2 S_{ii}(Q)+2z^{1/2}f_i(Q)S_{ie}(Q). \quad (5)$$

It may also be added that the order of magnitude of $\rho(Q)/2f_i(Q)$ is close to the value of $z/(2Z)$ and usually small, for example 0.10 for liquid aluminum in the Q range less than 100 nm^{-1} [12].

$\rho(Q)$ in eq.(4) is convenient for discussing the local charge density around an ion [17], while $S_{ie}(Q)$ in eq.(5) is useful to describe the electron distribution around an ion in liquid metals. The ion-ion partial structure factor provides the correlation function among the central point of ions and the form factor $f_i(Q)$ should be attributed to the spatial extent of ions. Thus, it is quite reasonable to assume that the center of ion is located at its nucleus and, therefore, the partial structure factor of ion-ion pairs $S_{ii}(Q)$ can be replaced by the neutron structure factor of $S_N(Q)=I_N^{\text{coh}}(Q)/Nb^2$, where $I_N^{\text{coh}}(Q)$ is the coherent neutron scattering intensity and b is the scattering length of neutrons [4]. Therefore, the conduction electron distribution in the momentum space $\rho(Q)$ could be expressed by,

$$\rho(Q) = \frac{[b^2 I_x^{\text{coh}}(Q)/I_N^{\text{coh}}(Q) - (f_i(Q))^2]}{2f_i(Q)} \quad (6)$$

When the values of $f_i(Q)$ are available, the estimation of $\rho(Q)$ is straightforward. The theoretical ionic form factor $f_i(Q)$ is usually given by the Hartree-Fock method [18] and it is possible to estimate from the X-ray scattering measurements for the ionic crystals [19]. Good agreement in these theoretical and experimental values is well appreciated in many cases [16].

Compare eq.(4) with eq.(4'), we obtain,

$$S_{ie}(Q) = (\rho(Q)/z^{1/2})S_{ii}(Q), \quad (7)$$

$$\rho(Q) = z^{1/2} \frac{S_{ie}(Q)}{S_{ii}(Q)}. \quad (8)$$

Thus, partial structure factor of ion-electron pair, $S_{ie}(Q)$, can readily be converted into $\rho(Q)$ using eq.(7), or vice versa. An equivalent formula was also presented by Petrillo and Sacchetti[20].

Based on the relation of eq.(4'), one can readily obtain the following equation, with respect to the ion-electron partial structure factor in liquid metals.

$$S_{ie}(Q) = [2z^{1/2}f_i(Q)]^{-1} [I_x^{\text{coh}}(Q) - f_i^2(Q)S_N(Q) - zS_{ee}(Q)]. \quad (9)$$

This equation corresponds to the starting equation to describe binary mixtures of ions and valence electrons in monatomic liquid metals in connection with measured structural data of X-rays and neutrons [9-12]. The partial structure factor of electron-electron pairs, $S_{ee}(Q)$, has long been well-studied for various densities of conduction electrons for example, the results of Utsumi-Ichimarū scheme [8]. In the present case, the distribution of valence electrons is considered to be the electron jellium in metallic density as the first approximation and it is relatively easy to calculate $S_{ee}(Q)$. Nevertheless, it is rather worth mentioning that there is no significant discrepancy in the numerical estimation of $S_{ie}(Q)$ from measured structural data using eq.(9), when the $S_{ee}(Q)$ term is excluded, because the values of $zS_{ee}(Q)$ are considerably smaller than those of $I_x^{\text{coh}}(Q)$ and $f_i^2(Q)S_N(Q)$ for Q range of the present interest. Thus, eq.(9) is in practice, approximated by the following form with respect to $S_{ie}(Q)$.

$$S_{ie}(Q) = [2z^{1/2}f_i(Q)]^{-1} [I_x^{\text{coh}}(Q) - f_i^2(Q)S_N(Q)]. \quad (10)$$

The corresponding partial radial distribution function $g_{ie}(r)$ is readily obtained by the following Fourier transformation.

$$g_{ie}(r) = 1 + \frac{1}{2\pi^2 \rho_0 r^2} \int_0^\infty z^{-1/2} S_{ie}(Q) Q \sin(Qr) dQ, \quad (11)$$

where $\rho_0 = zN/V_M$, V_M and N are the molar volume and the Avogadro's number, respectively.

3. Ion-Electron Correlations in Several Liquid Metals

The structure factors for several liquid metals were now determined by neutron diffraction with sufficient accuracy [9-12] and then significant difference from the structure factors obtained by X-ray diffraction [14] has been well recognized, as exemplified by Fig.1 using the results of liquid sodium where the qualitative coincidence appears with respect to the structural profile [10]. The quantity of $[S_X(Q) - S_N(Q)]$ calculated from two structure factors are given in Fig.2. It may be a help to see the well-appreciated systematic difference and oscillating profile in the quantity of $[S_X(Q) - S_N(Q)]$. Here, two X-ray diffraction results, independently obtained by different research group of Netherlands [21] and Japan [14], were used for comparison with the neutron case. It is intention of the present authors to stress that the essential agreement

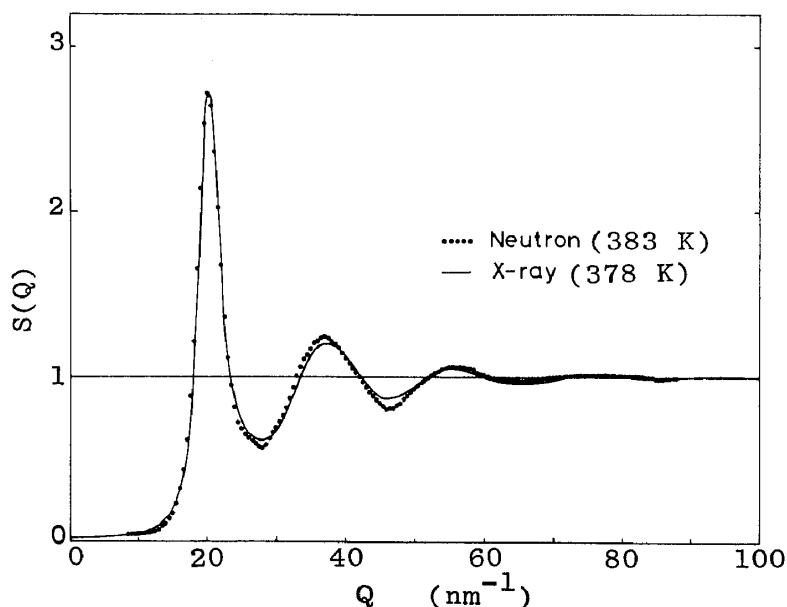


Fig.1 Structure factors of liquid sodium determined by X-ray (solid line) and neutron (dotted line) diffraction [10].

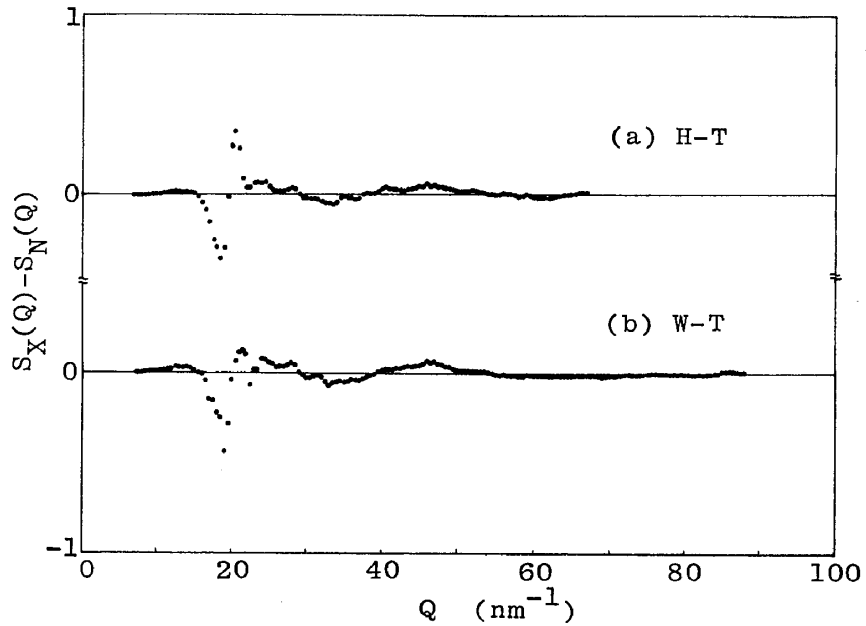


Fig.2 Structural profiles of $[S_X(Q) - S_N(Q)]$ for liquid sodium. (a): X-ray diffraction is taken from the data of Huijben and van der Lugt [21]. (b) X-ray diffraction is taken from the data of Waseda [14].

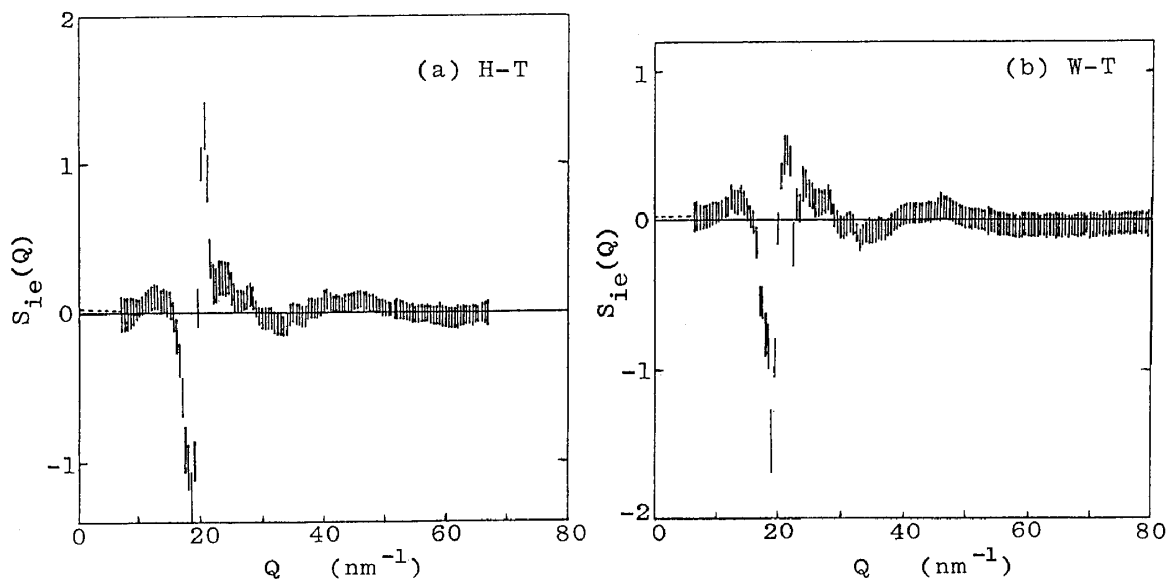


Fig.3 Partial structure factor of ion-electron pairs in liquid sodium. (a): X-ray diffraction is taken from the data of Huijben and van der Lugt [21]. (b) X-ray diffraction is taken from the data of Waseda [14].

is very much encouraging in these two sets of structural data, independently obtained by different research groups using X-ray diffraction, although there are some differences in detail.

Along the line of the relatively new procedure with eq.(10), the ion-electron correlation functions of $S_{ie}(Q)$ can be estimated from measured structural data. The results of liquid sodium are illustrated in Fig.3 [10]. The vertical lines in this figure indicate the experimental uncertainty which is of the order of ± 0.2 estimated from the counting statistical errors of intensity measurements of x-rays and neutrons. Such scatter arises mainly from the fact that the difference between $S_X(Q)$ and $S_N(Q)$ is relatively small in comparison with the uncertainties of S_X and $S_N(Q)$ themselves and a serial test using the computer technique of numerical calculation also confirms the significance of principal profile of these functions. We found again good coincidence in these two sets of data, except for the difference of the positive amplitude of the oscillations in the region of $Q=20 \text{ nm}^{-1}$. The difference in the structure factors between $S_X(Q)$ and $S_N(Q)$ disappear beyond about $Q=55 \text{ nm}^{-1}$ as shown in Fig.3 and the atomic form factor $f_a(Q)$ is in accord with

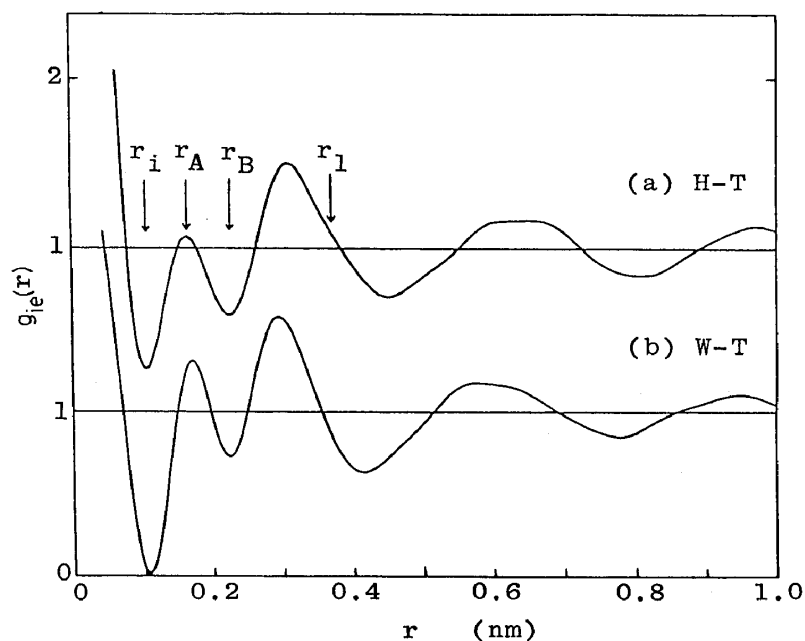


Fig.4 Partial radial distribution function of ion-electron pairs in liquid sodium. (a): X-ray diffraction is taken from the data of Huijben and van der Lugt [21]. (b) X-ray diffraction is taken from the data of Waseda[14]. r_i : ionic radius, r_A : first maximum position of $g_{ie}(r)$, r_B : first minimum position of $g_{ie}(r)$, in the range between the neighbor ions, r_1 : distance of the nearest neighbor ions.

tion functions are exemplified by Fig.5 using the results of liquid zinc, tin and bismuth. Some interesting and important observation could be made from these data about the valence electron distribution around an ion for polyvalent liquid metals.

As easily seen in Fig.5, a sharp drop of distribution function occurs at a certain small value of r . For example, the $g_{ie}(r)$ curve drops at the distance of 0.074 nm for zinc, 0.072 nm for tin and 0.075 for bismuth, which exactly agree with the well-known ionic radii proposed by Pauling [22], as summarized in Table 1. This a-

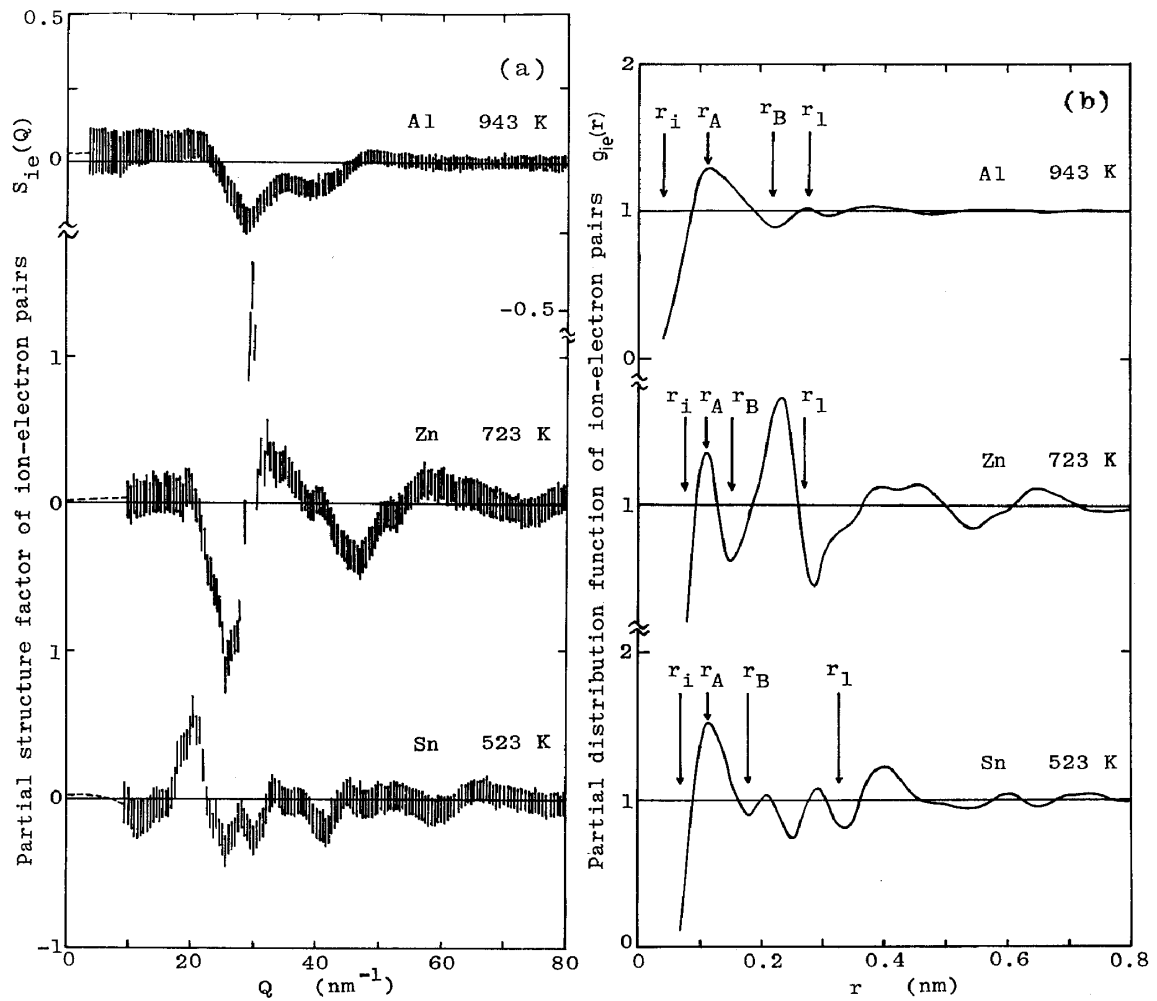


Fig.5 Partial structure factor $S_{ie}(Q)$ and partial radial distribution function $g_{ie}(r)$ of ion-electron pairs in liquid aluminum, zinc and tin [10,12]. r_i : ionic radius, r_A : first maximum position of $g_{ie}(r)$, r_B : first minimum position of $g_{ie}(r)$, in the range between the neighbor ions, r_1 : distance of the nearest neighbor ions.

reement for ionic radius is, from present authors' view, rather surprisingly good. The number of valence electrons localized at the close vicinity of an ion, n_{ve} , can also be calculated from the area under the first peak of the $4\pi r^2 g_{ie}(r)$ curve given in Fig.6 using the result of liquid zinc as an example. The n_{ve} value is estimated to be 1.7 for zinc and this suggests that most of valence electrons (1.7) associate with ions and remainders (0.3) exist in the intermediate region among ions, because the valence electron number is well-known to be 2 for zinc. For convenience, the n_{ve} values obtained for other metals are summarized in Table 1. It may be added that the different localization of valence electrons is suggested among aluminum, gallium and thallium or between tin and lead for elements having the same valence number [9,10].

On the other hand, another noticeable feature is clearly found in the valence electron distribution around an ion in liquid sodium. As easily seen in Fig.3, the $g_{ie}(r)$ curve of liquid sodium increases sharply with decreasing the distance inside of r_i , which contrasts with the polyvalent metal cases given in Fig.5. The present authors maintain the view that this is probably attributed to the penetra-

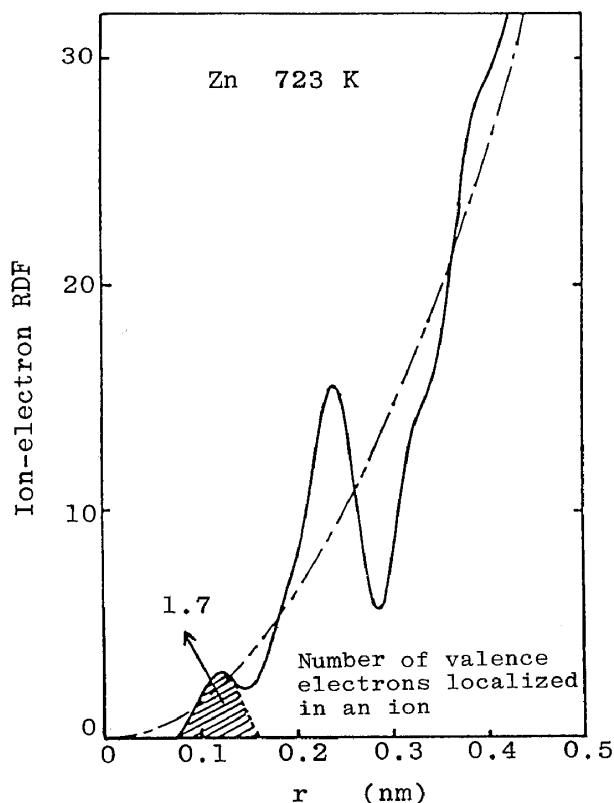


Fig.6 Ion-electron RDF of liquid zinc. Hatched area corresponds to the number of valence electrons closely located around an ion [10].

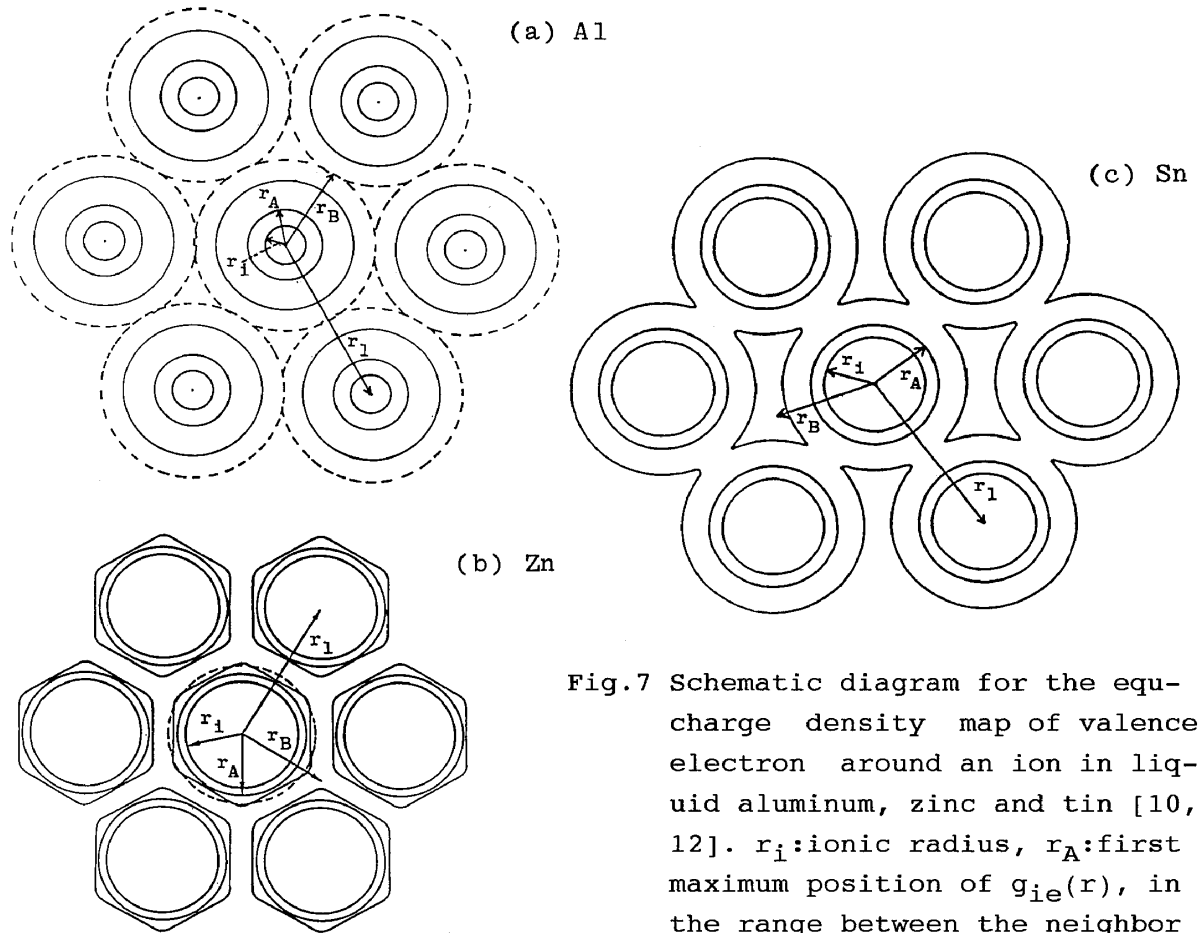


Fig.7 Schematic diagram for the equ-charge density map of valence electron around an ion in liquid aluminum, zinc and tin [10, 12]. r_i :ionic radius, r_A :first maximum position of $g_{ie}(r)$, in the range between the neighbor ions, r_1 :distance of the nearest neighbor ions.

Table 1 Ionic radius r_i and its relevant information obtained from the ion-electron correlation functions experimentally determined in unit of nm. n_{ve} : number of valence electrons localized in an ion [10,12].

	r_i	ionic radius (Pauling)	r_A	r_B	r_1	n_{ve}
Na ⁺	0.105	0.095	0.165	0.225	0.381	0.7
Zn ²⁺	0.074	0.074	0.110	0.141	0.268	1.7
Al ³⁺	0.045	0.050	0.115	0.225	0.282	2.8
Ga ³⁺	0.070	0.062	0.118	0.156	0.282	2.2
Tl ³⁺	0.080	0.095	0.110	0.143	0.328	0.9
Sn ⁴⁺	0.072	0.071	0.096	0.167	0.323	2.7
Pb ⁴⁺	0.080	0.084	0.108	0.160	0.333	1.9
Bi ⁵⁺	0.075	0.074	0.094	0.172	0.338	1.5

tion of electron charge from outside to the inside of the ion core [10]. Thus, it may be, more or less that eq.(10) is not sufficient enough for completely describing the distribution of ions and valence electrons in liquid metals, where the electron charge distributes both outside and inside of the ion core. It may be worth mentioning that this characteristic feature found in liquid sodium is consistent with the recent theoretical calculation of liquid lithium by Chihara [15].

The partial radial distribution function of ion-electron pairs enables us to provide the inhomogeneous distribution of valence electrons surrounding ions in liquid metals, because the first peak of $g_{ie}(r)$ for respective liquid metals is likely corresponding to the distribution of the electron cloud around an ion located at the origin and the second peak means the electron cloud around the neighboring ions. Thus, the spatial distribution of the valence electrons around ions in liquid metals may be schematically given by drawing the equi-charge density map. The equi-charge density map in liquid metals are illustrated in Fig.7 for liquid aluminum, zinc and tin. Here, the fcc type structural coordination is considered for aluminum and zinc, whereas the bcc type is employed for tin, using the experimental data of the coordination number in the nearest neighbor region determined from the ordinary RDF data of ion-ion pairs. The following observations could be made from these equi-charge density map of the valence electrons around an ion in liquid metals [9-12]. These information may also be of interest, because all of the liquid metals can be put into one of the three types; that is, having structures similar to those of aluminum, zinc and tin as exemplified by the structure factors of Fig.8 [14].

The ratio between the ionic diameter of Zn^{2+} (0.148 nm) and the nearest neighbor ion-ion distance (0.268 nm) is much larger than those of other liquid polyvalent metals (see Table 1) and the valence electron distribution is relatively close packed. Then, the equi-charge density line near the lowest charge density region produces the deformation from the spherical surface, as shown in Fig.7(b). This deformation seems to be related to the characteristic asymmetry of the first peak of the structure factor for liquid zinc (see Fig.8). Such deformation arising from the harmony of the valence electron distribution and the nearest neighbor ion-ion distance is considered not to severely depend on temperature. This is consistent with the experimental fact that the asymmetric nature of the first peak for the Zn type liquid metals remains at higher temperatures [14].

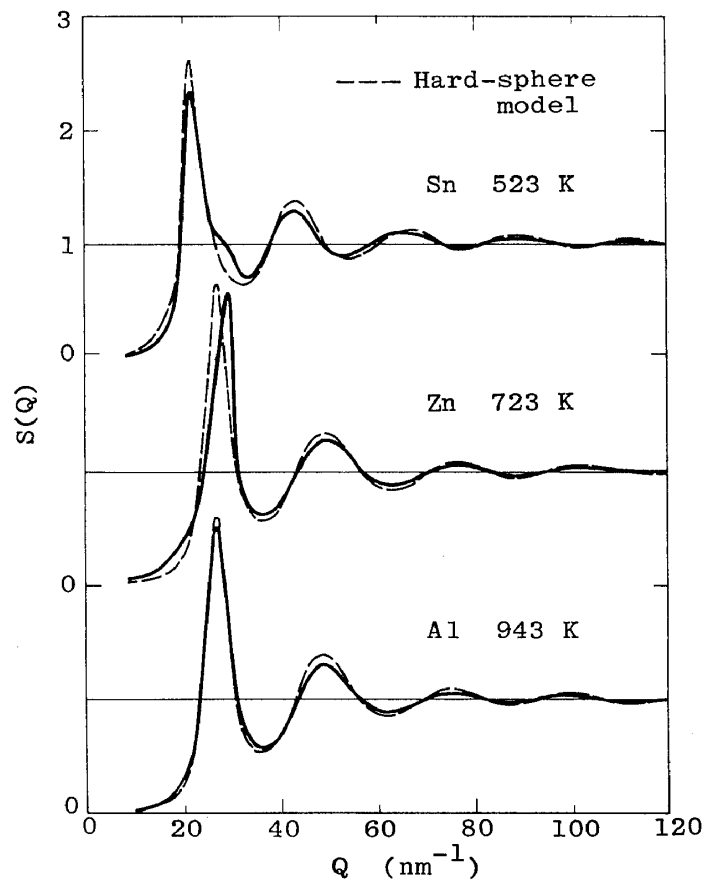


Fig.8 Structure factors of liquid aluminum, zinc and tin near the melting point with hard sphere structure factor for comparison [14].

In the case of liquid tin, the electron cloud of valence electrons surrounding ions is found to be at 0.096 and 0.22 nm. Since the nearest neighbor ion-ion distance is known to be 0.323 nm, the minimum value may be expected in the close vicinity of $r=0.32$ nm. Then, the valence electrons more than the average density are spread out over the nearest neighbor ions in liquid tin and there exists the relatively large space of lower density region, as given in Fig.7(c). As discussed in previous works[23-25], the ledge-type repulsion is quite feasible in the effective pair potential of liquid tin and bismuth with respect to the small hump on the high angle side of the first peak in their structure factors and it may correspond to the existence of shorter interionic interaction component, in addition to the average nearest neighbor distance.

The co-existence of such shorter interionic interaction component, in contrast to the average nearest neighbor interaction distance (r_1) is suggested in the tin type liquid metals, with respect

to the characteristic small hump on the high angle side of the first peak (see Fig.8). A small shoulder on the right hand side of the first peak in $g_{ie}(r)$ is likely reflected upon such a shorter inter-ionic interaction component in liquid tin, because the electron cloud relevant to the small shoulder is able to screen a strong Coulomb repulsion between ions located in the near neighbor region. The inhomogeneous distribution of valence electrons including the relatively large space of lower density at about the midpoint between the nearest neighbor ions in liquid tin seems to be one of the origins attributed to the characteristic small hump on the high angle side of the first peak in its structure factor. It may also be noticed that the relatively large space of lower density is diminished when the ionic vibrations increase at higher temperature. This should be related to the disappearance of the small hump of the tin type liquid metals [14].

Compared with the characteristic features found in the inhomogeneous distribution of the valence electrons around an ion for liquid zinc and tin, the rather symmetrical nature is well-recognized in the valence electron distribution map for liquid aluminum [12], although the valence electrons are distributed with the relatively low density around ions, as shown in Fig.7(a). This symmetrical nature in the ion-electron correlations can most likely attributed to the simple structural features for the aluminum type liquid metals (see Fig.8). It is worth mentioning, from the results of other liquid metals using the same procedure, that the electron distribution map of liquid gallium and bismuth is essentially classified into the tin case and liquid sodium, thallium and lead show the electron distribution map similar to the aluminum case, although there are differences in detail [9-12].

4. Electron Charge Distribution Function in Liquid Metals

As described in section 2, the electron charge distribution function, $\rho(Q)$ in the momentum space, can also be estimated from measured structural data using eq.(6). Such information of $\rho(Q)$ is exemplified by Fig.9 using the result of liquid aluminum for example [12]. Here, we use the form factor $f_i(Q)$ compiled in the International Tables for X-ray Crystallography [16]. The vertical lines in this figure denote the experimental uncertainties. The calculation of the electron charge distribution in the real space $\rho(r)$ is simply made by the usual Fourier transformation. For this purpose,

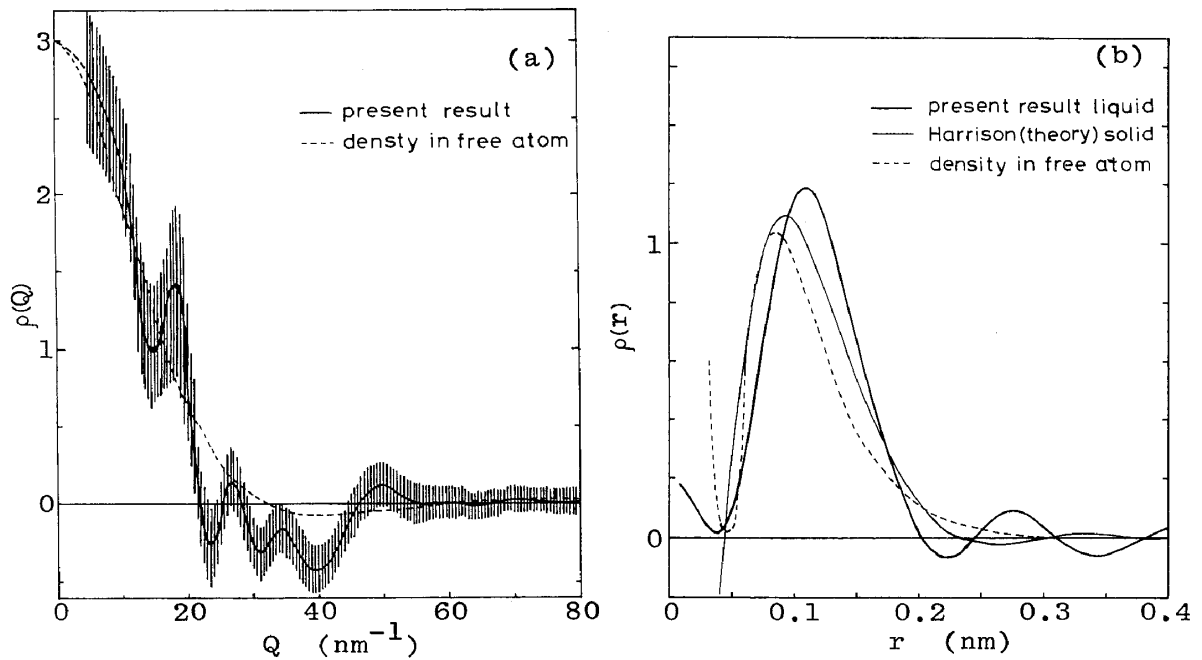


Fig.9 Electron charge distribution functions of liquid aluminum in the momentum space (a) and in the real space (b) [12].

the profiles of $\rho(Q)$ were assumed to be a smooth function; thus the average values at each Q were employed. The resultant $\rho(r)$ is given in Fig.9(B) together with the results estimated by Harrison [17] using the pseudo-potential method. The density distribution in free atom is also illustrated for convenience.

As shown in Fig.9(B), the agreement of two curves calculated by the pseudo-potential method and estimated from measured structural data is rather surprisingly good, from both qualitative and quantitative point of view, except for the behavior in the core region. This exception is considered to be acceptable, because the behavior of electrons is treated as a nearly free one even in the core region in the pseudo-potential theory [17]. If the wave function of conduction electrons is expressed, for example, as in the orthogonal plane wave (OPW) form [17,18], then the conduction electrons would most likely behave as the atomic wave function in the close vicinity to the ionic radius. This suggests that a sharp increase toward the center of an ion in $\rho(r)$ may be attributed to the mixing effect of a part of the conduction electrons with the outer core electrons of ions concerned. However, it is also noteworthy to stress that there is only small fraction of such conduction electrons in the range less than 0.05 nm, because the conduction electron distribution follows the form of $4\pi r^2 \rho(r)$. Therefore, the valence electrons in

liquid aluminum appear most likely behave as nearly free, except for a minor OPW effect. A similar behavior of $\rho(r)$ in liquid metals has also been obtained for liquid sodium [11].

5. Concluding Remarks

The ion-electron correlation functions in liquid metals given in this article should be considered to include some reservation and the direct estimation of the valence electron distribution around an ion in liquid metals from measured structural data of X-rays and neutrons is far from complete. However, the selected examples clearly indicate the inhomogeneous distribution of valence electrons surrounding ions, in harmony with the ionic distribution in liquid metals and they are found to be consistent with the characteristic structural features, such as the asymmetry of the first peak in liquid zinc or the small hump on the high angle side of the first peak in liquid tin which have long been suggested. Thus, the present authors take the view that the relatively new method given here represent, at least, one possible way and one step forward for experimentally obtaining information on the fundamentals of the valence electron distribution in liquid metals directly from measured x-ray and neutron diffraction data.

It would be interesting, although undoubtedly more difficult, to extend the present method to other liquid metals, particularly liquid transition metals and rare earth metals. There remains much work to be done in preparing accurate form factors and diffraction data of neutrons for these liquid metals, but such further efforts may also test the usefulness and validity of the present method on a wider basis.

References

1. S.Ichimaru: Rev. Mod. Phys., **54**(1982),1017.
2. M.Watabe and M.Hasegawa: Proc. 2nd Inter. Conference on Liquid Metals, ed. S.Takeuchi, Taylor and Francis, London, (1973), p.133.
3. J.Chihara: Proc. 2nd Inter. Conference on Liquid Metals, ed. S.Takeuchi, Taylor and Francis, London, (1973), p.137.
4. P.A.Egelstaff, N.H.March and M.C.McGill: Can. J. Phys., **52**(1974),1651.

5. P.J.Dobson: J. Phys. C. Solid State Phys., 11(1978),L295.
6. H.Olbrich, H.Ruppersberg and S.Steeb: Zeit. fur Naturforsch., 38a(1983),1328.
7. S.Cusack, N.H.March, M.Parinello and M.P.Tosi: J. Phys. F. Metal Phys., 6(1976),749.
8. K.Utsumi and S.Ichimaru: Phys. Rev., 22(1980),5203.
9. S.Takeda, S.Tamaki and Y.waseda: J. Phys. Soc. Japan, 54(1985),2552.
10. S.Takeda, S.Harada, S.Tamaki and Y.waseda: J. Phys. Soc. Japan, 55(1986),184; *ibid.*, 55(1986),3437; *ibid.*, 58(1989),3999.
11. S.Takeda, S.Tamaki and Y.Waseda: J. Phys. Cond. Matter, 2(1990),6451.
12. S.Takeda, S.Harada, S.Tamaki and Y.Waseda: J Phys. Soc. Japan, 60(1991),2241.
13. N.W.Ashcroft and D.C.Langreth: Phys. Rev., 159(1967),500.
14. Y.Waseda: The Structure of Non-Crystalline Materials, McGraw-Hill, New York, (1980).
15. J.Chihara: J. Phys. F. Matal Phys., 17(1987),295.
16. International Tables for X-ray Crystallography, Vol.IV, ed. J.A.Ibers and W.C.Hamilton, The Kynoch Press, Birmingham (1974).
17. W.A.Harrison: Pseudopotentials in the Theory of Metals, Benjamin, New York, (1966).
18. J.M.Ziman: Principles of the Theory of Solids, Cambridge Univ. Press, (1965).
19. R.W.James: The Optical Principles of the Diffraction of X-rays, G.Bell & Sons, London, (1954).
20. C.Petrillo and F.Sachetti: J. Phys. F. Metal Phys., 16(1986),L283.
21. M.J.Huijben and W. van der Lugt: Acta Cryst., A35(1979),431.
22. L.Pauling: The Nature of the Chemical Bonds, Cornell Univ. Press, Ithaca, New York, (1939).
23. M.Silbert and W.H.Young: Phys. Letter, 58A(1976),469.
24. K.K.Mon, N.W.Ashcroft and G.V.Chester: Phys. Rev., B19(1979),5103.
25. S.Takeda, S.Tamaki and Y.Waseda: J. Phys. Soc. Japan, 53(1984),3447.